

Supporting Information

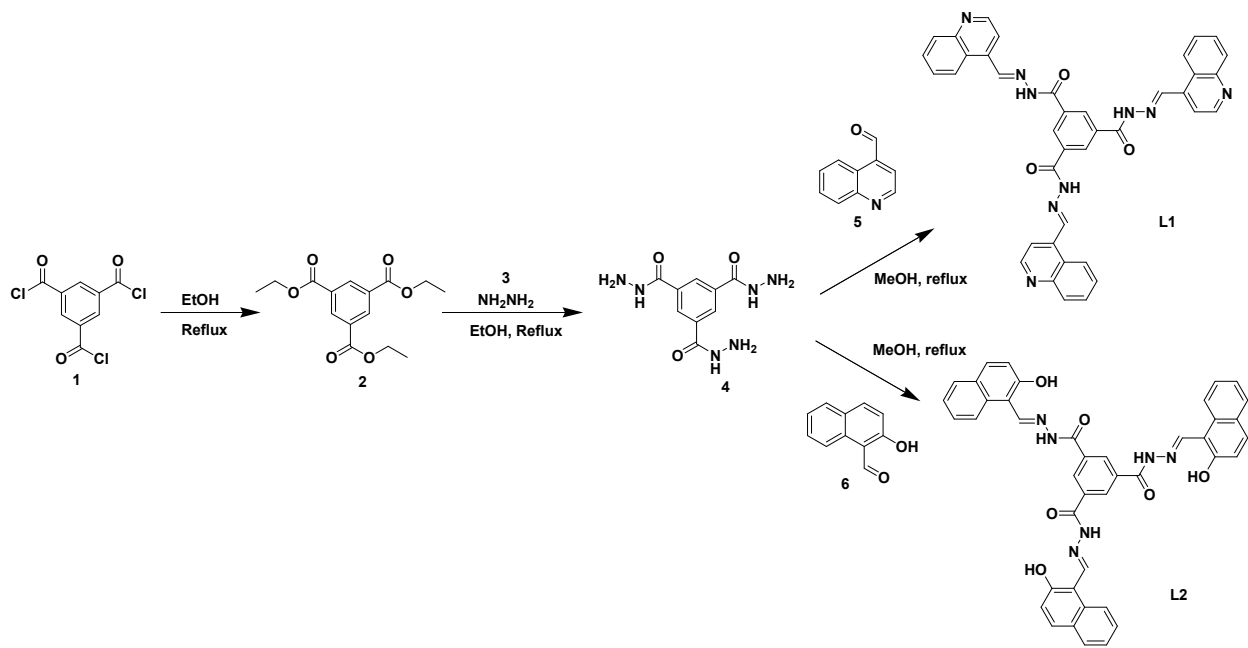
C₃-Symmetrical Tripodal Acylhydrazone Organogelator for the Selective Recognition of Cyanide ions in Gel and Solution phase: Practical Applications in Food Samples

Shilpa Sharma, Manisha Kumari, Narinder Singh*

Department of Chemistry, Indian Institute of Technology Ropar, Rupnagar, Punjab 140001, India

Corresponding Author: nsingh@iitrpr.ac.in

S. No.	Content	Page number
1.	Synthesis routes for the synthesis of ligand L1 and ligand L2	S2
2.	¹ H NMR Spectrum of Ligand L1	S3
3.	HRMS spectrum of Ligand L1	S3
4.	¹³ C NMR Spectrum of Ligand L1	S4
5.	FTIR spectra of Ligand L1	S4
6.	¹ H NMR Spectrum of Ligand L2	S5
7.	HRMS spectrum of Ligand L2	S5
8.	¹³ C NMR Spectrum of Ligand L2	S6
9.	FTIR spectra of Ligand L2	S6
10.	Gelation behaviors at room temperature	S7
11.	FT-IR spectrum of the powder of ligand L1 and organogelator L1	S7
12.	Time dependence fluorescence emission spectra of ligand L1 (90:10, H ₂ O:DMSO) at 480 nm.	S8
13.	Fluorescence emission spectra of ligand L2 (10 μM) in different DMSO: H ₂ O ratios.	S8
14.	UV-Vis. absorption spectra of ligand L1 (10 μM) in DMSO	S9
15.	Detection limit showing the absorbance of ligand L1 at 416 nm as a function of CN ⁻ ions concentration	S9
16.	UV-Vis. response of Ligand L1 to different anions.	S10
17.	Interference studies of Ligand L1	S10
18.	Time Response of Ligand L1 (100μM) upon addition of different equiv. of CN ⁻ ions	S11
19.	pH response of ligand L1 by varying pH from 3 to 10.	S11
20.	UV-Vis. absorption spectra of ligand L2 in DMSO.	S12
21.	UV-Vis. absorption spectra of ligand L2 upon addition of 15 equiv. of CN ⁻ ions.	S12
22.	The FT-IR spectrum of the organogelator L1 in presence of CN ⁻ ions.	S13
23.	The comparison of the ligand L1 for cyanide detection with other cyanide sensitive sensor	S13



Scheme 1. Synthesis routes for the synthesis of ligand **L1** and ligand **L2**

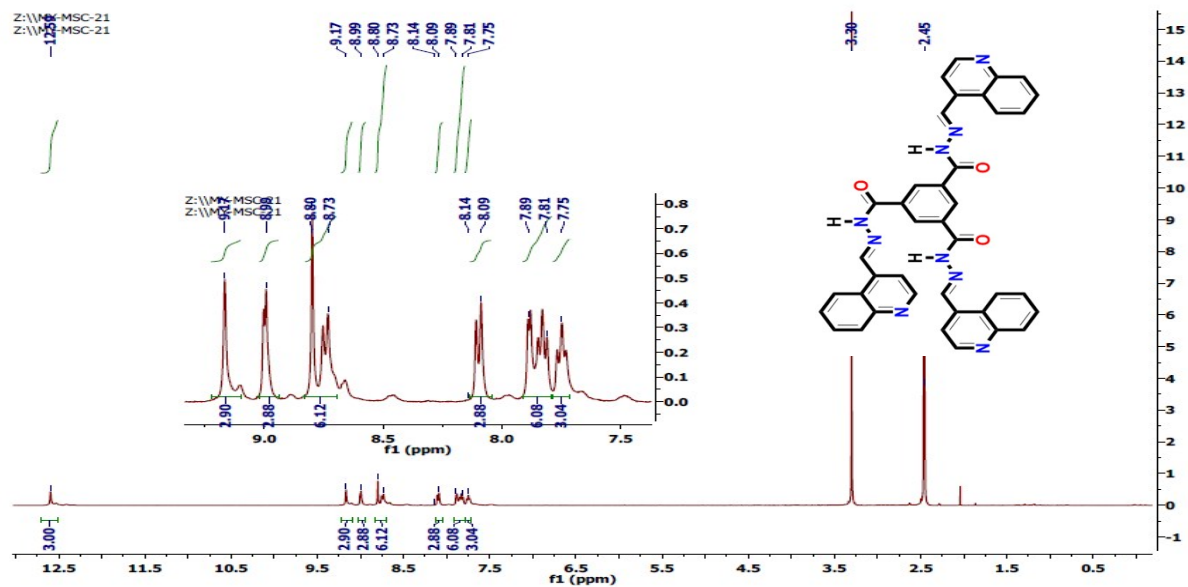


Fig. S1 ¹H NMR Spectrum of Ligand L1

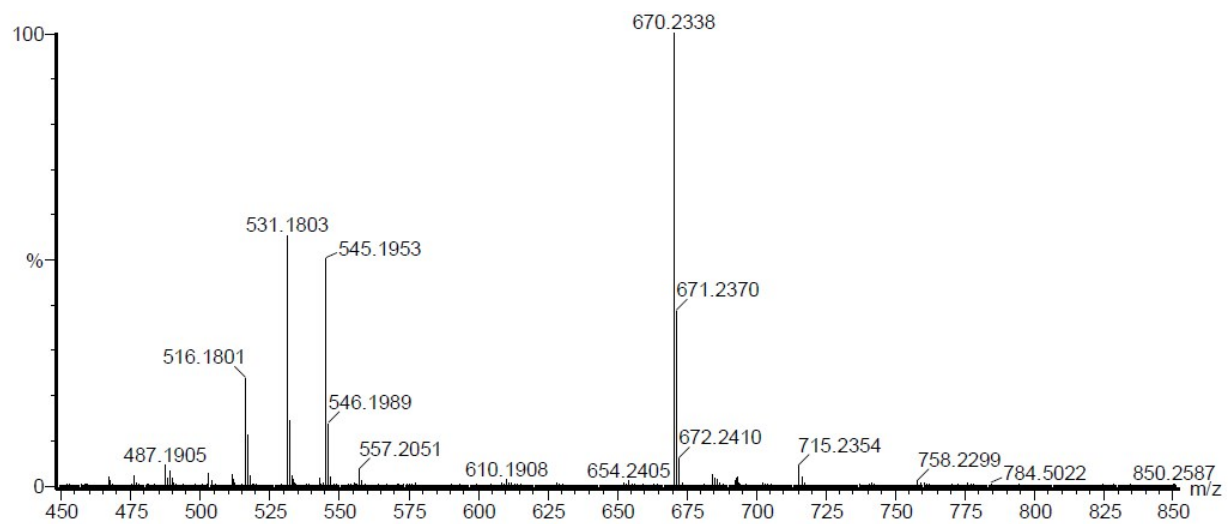


Fig. S2 HRMS spectrum of Ligand L1

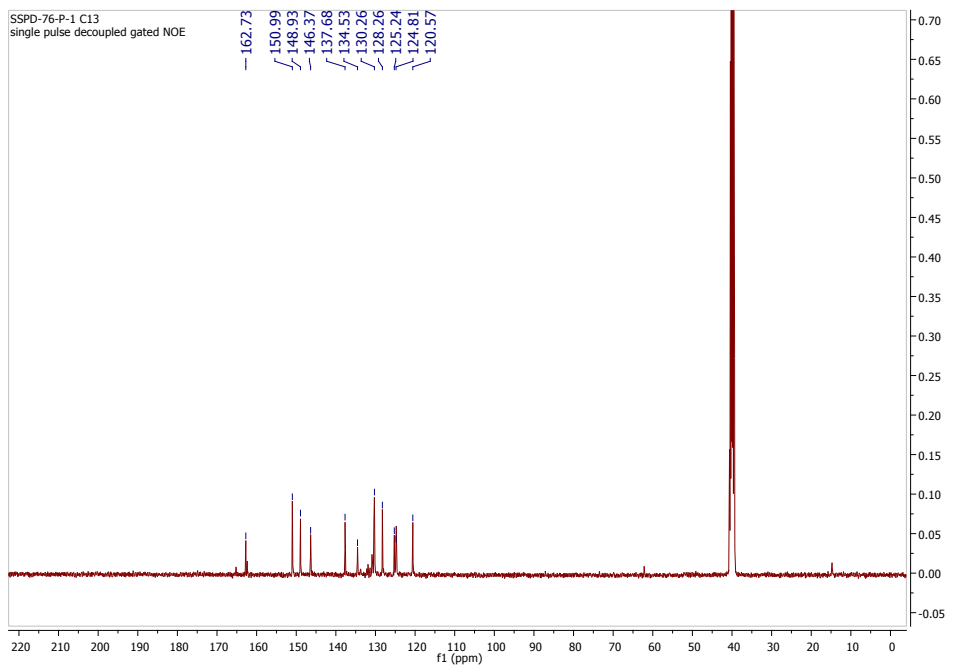


Fig. S3 ^{13}C NMR Spectrum of Ligand **L1**

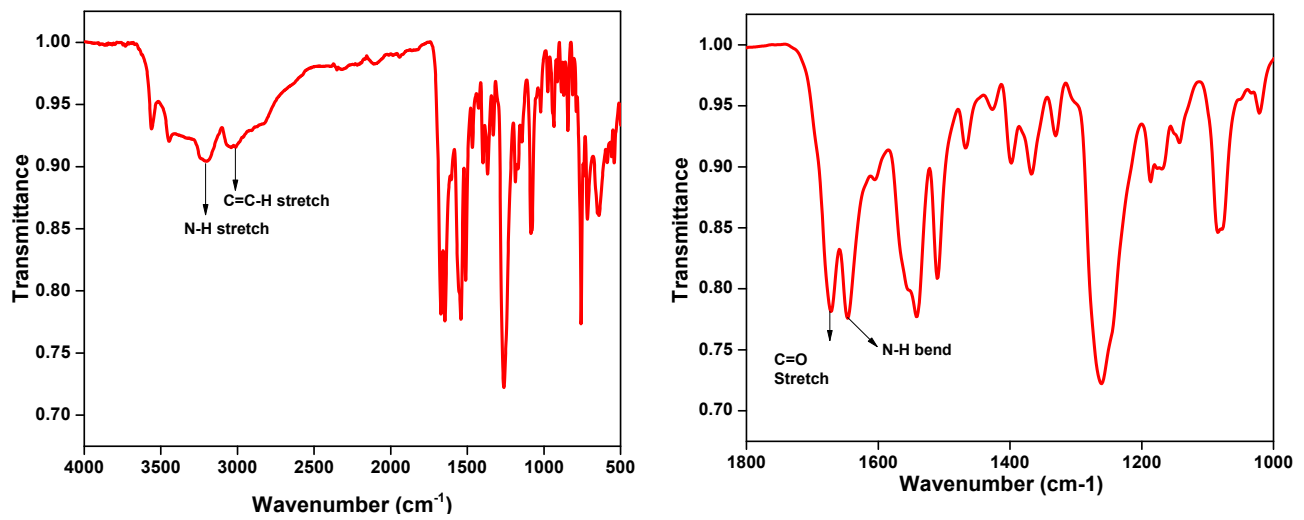


Fig. S4 FTIR spectra of Ligand **L1**

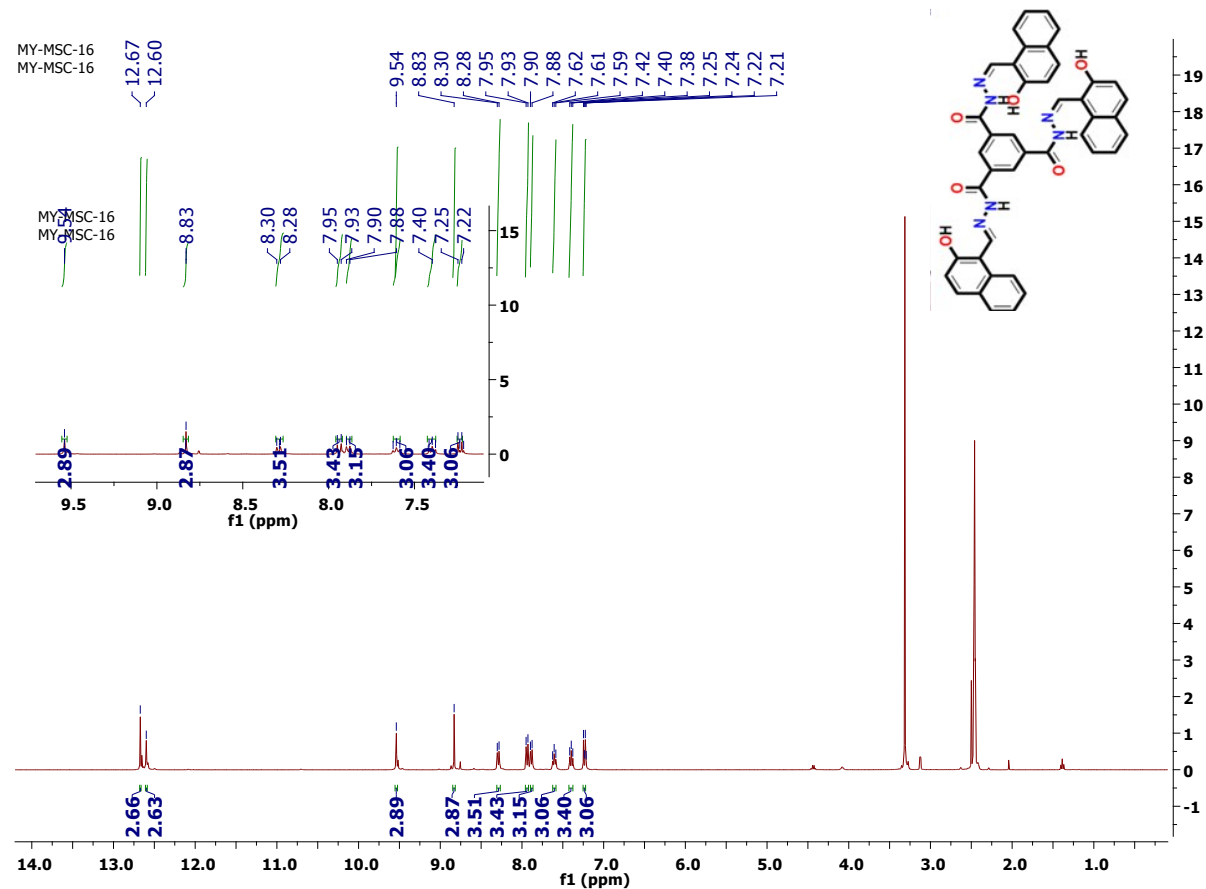


Fig. S5 ¹H NMR Spectrum of Ligand **L2**

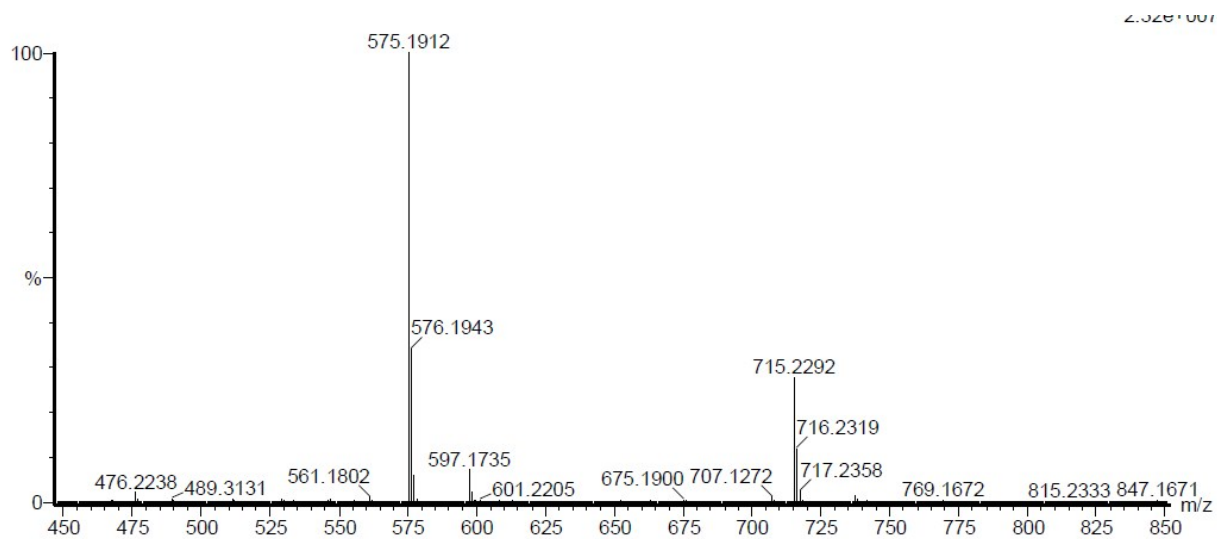


Fig. S6 HRMS spectrum of Ligand **L2**

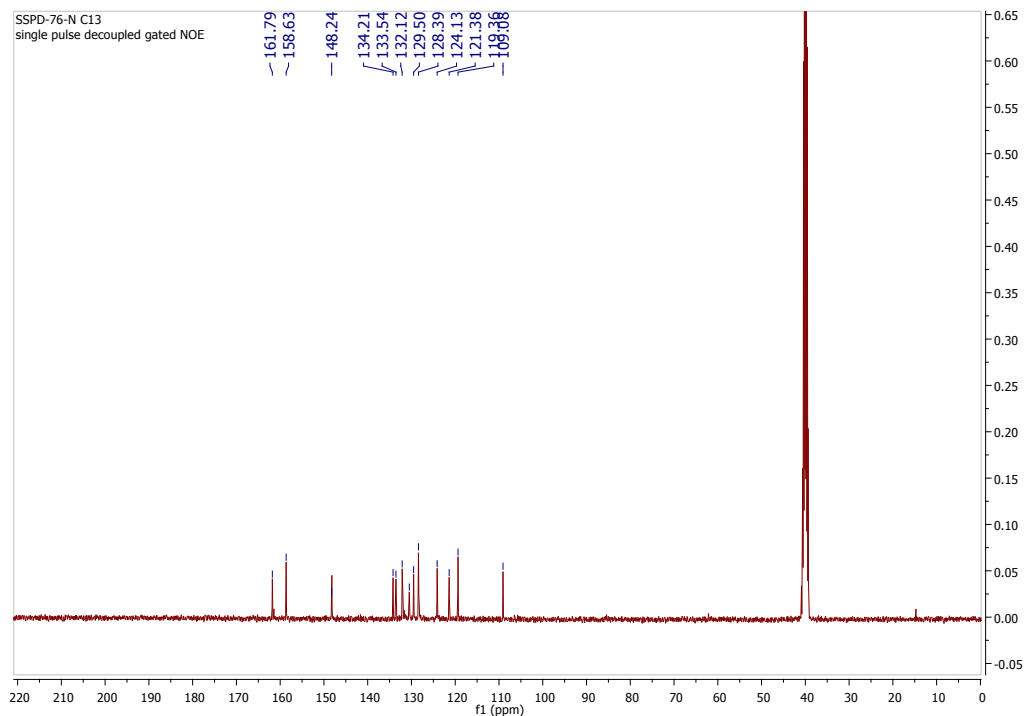


Fig. S7 ^{13}C NMR Spectrum of Ligand **L2**

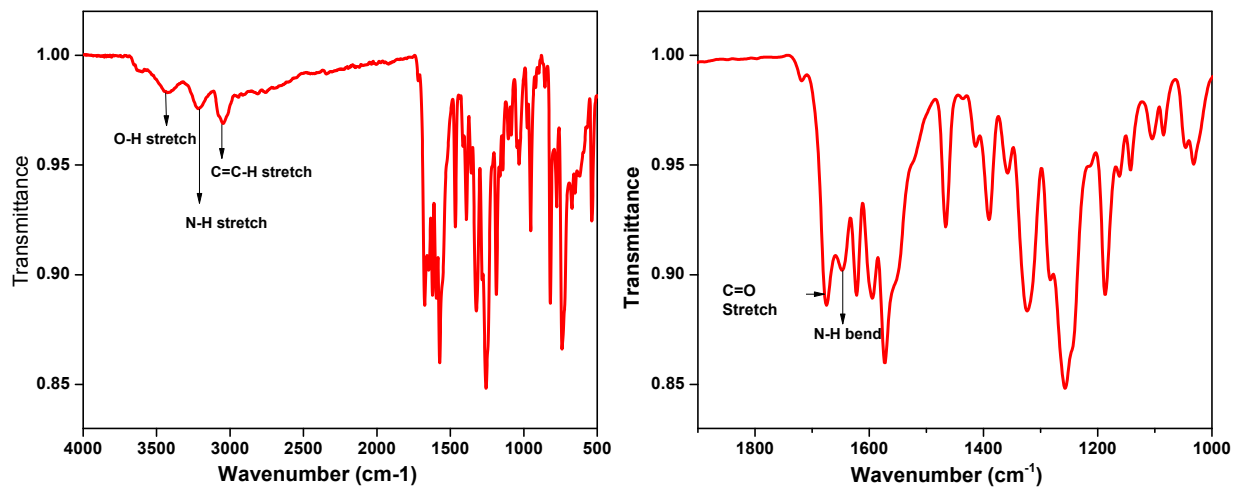


Fig. S8 FTIR spectra of Ligand **L2**

Table S1: Gelation behaviors at room temperature

S.No.	Solvent Ratio (DMSO: H ₂ O, v/v)	Ligand L1	Ligand L2
1.	1	9	I
2.	2	8	PS
3.	3	7	PS
4.	4	6	PS
5.	5	5	G
6.	6	4	PS
7.	7	3	S
8.	8	2	S
9.	9	1	S
10.	10	0	S

S: solution; PS: partially soluble; G: gel; I: insoluble; for gels

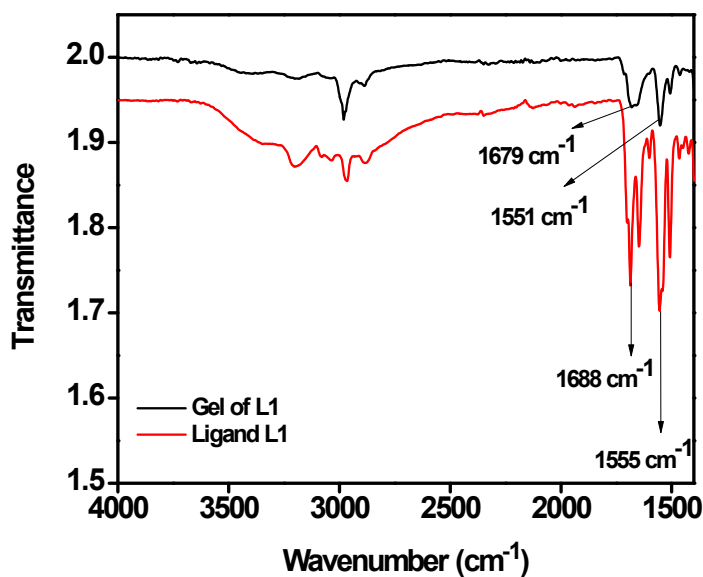


Fig. S9 FT-IR spectrum of the powder of ligand **L1** and organogelator **L1** in xerogel form.

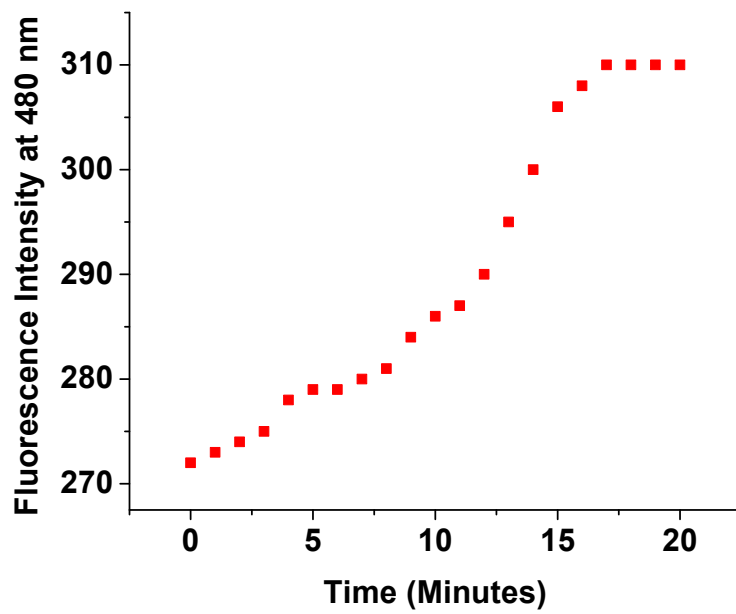


Fig. S10 Time dependence fluorescence emission spectra of ligand **L1** (90:10, H₂O:DMSO) at 480 nm.
(error)

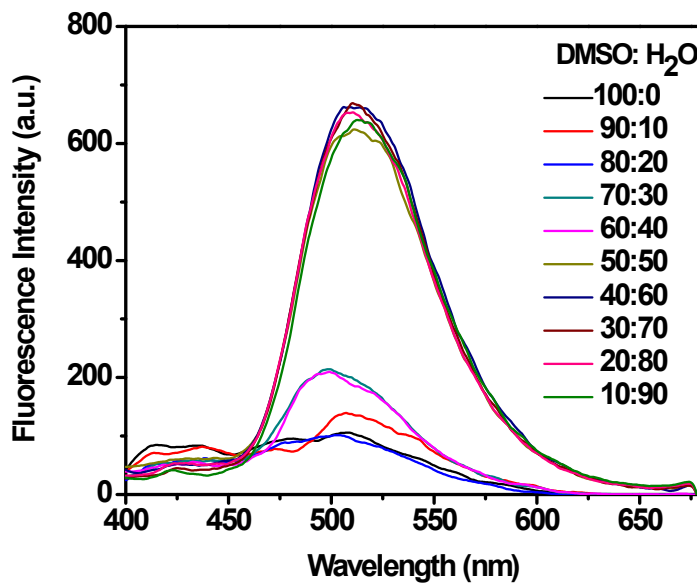


Fig. S11 Fluorescence emission spectra of ligand **L2** (10 μ M) in different DMSO: H₂O ratios.

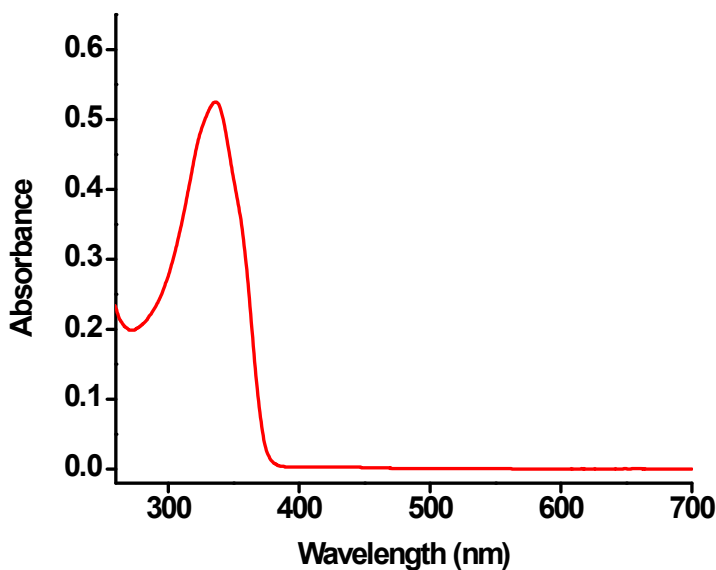


Fig. S12 UV-Vis absorption spectra of ligand **L1** (10 μM) in DMSO.

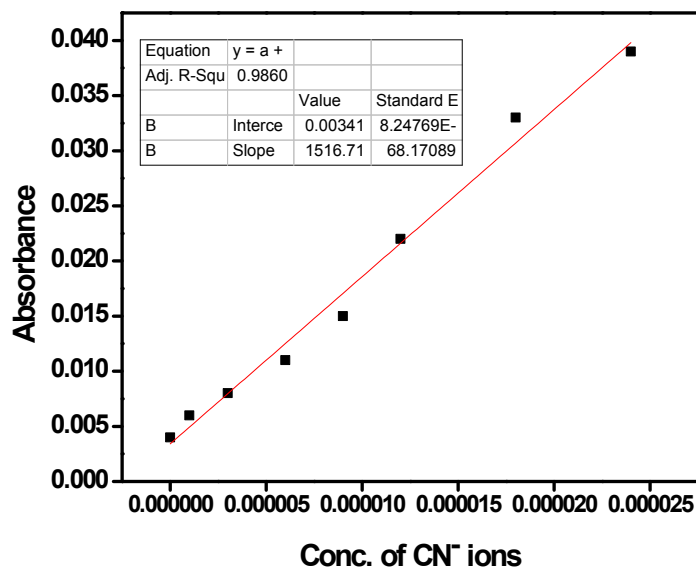


Fig. S13 Detection limit showing the absorbance of ligand **L1** at 416 nm as a function of CN^- ions concentration.

Table 2. Detection limit showing the absorbance of ligand **L1** at 416 nm as a function of CN^- ions concentration

S.no.		σ	M	$3\sigma/M$	Detection limit
1	ligand L1 +15 equiv. of CN^- ions	0.00079	1516.17	1.5×10^{-6}	1.5 μM

* σ = Standard deviation of the blank sample

*M = corresponds to slope of the regression line.

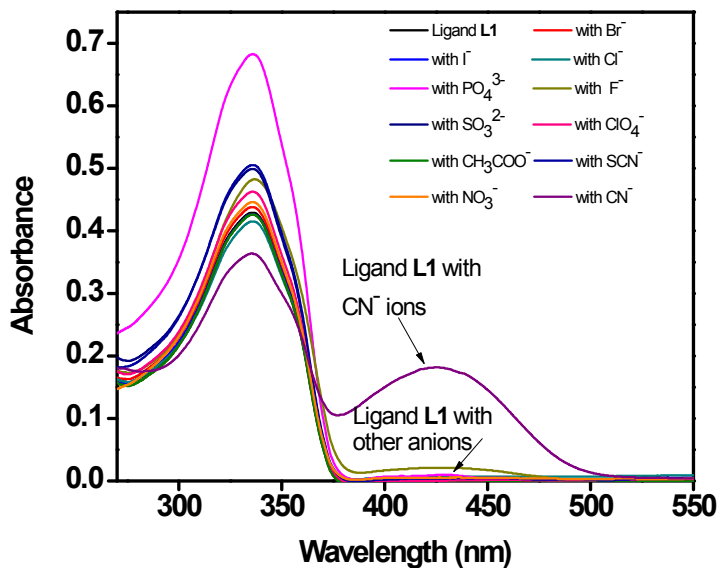


Fig. S14 UV-Vis response of Ligand **L1** to different anions

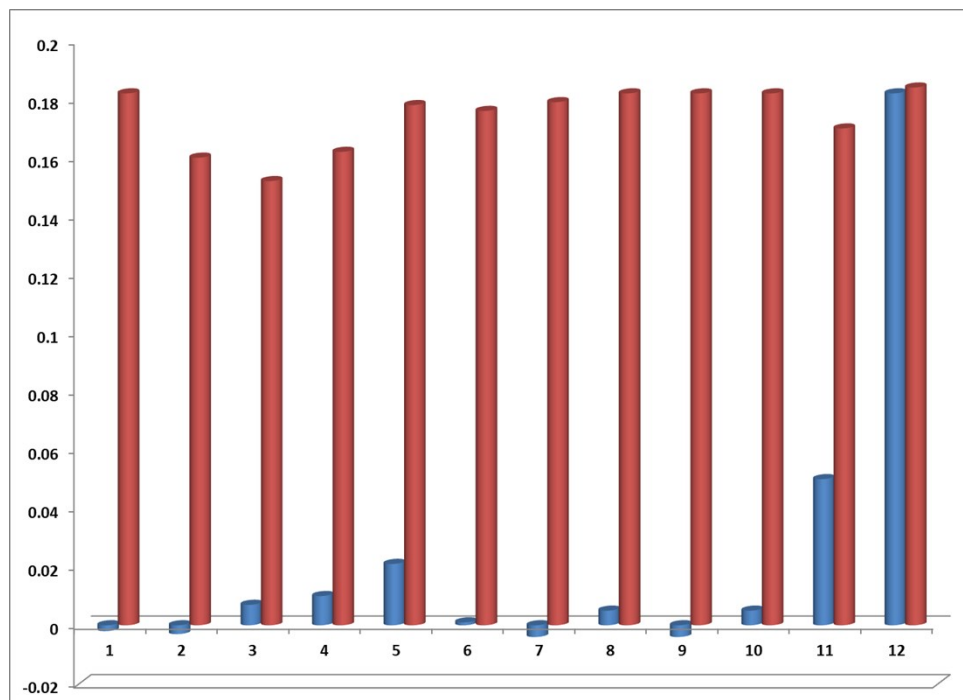


Fig. S15 Interference studies of Ligand **L1** ($10 \mu\text{M}$) upon addition 15 equiv. of different ions (shown by blue bars) followed by 15 equivalent CN^- ions (shown by red bars). Where 1) Ligand **L1** with 2) SCN^- 3) Br^- 4) I^- 5) Cl^- 6) PO_4^{3-} 7) NO_3^- 8) SO_3^{2-} 9) ClO_4^- 10) CH_3COO^- 11) F^- 12) CN^- ions.

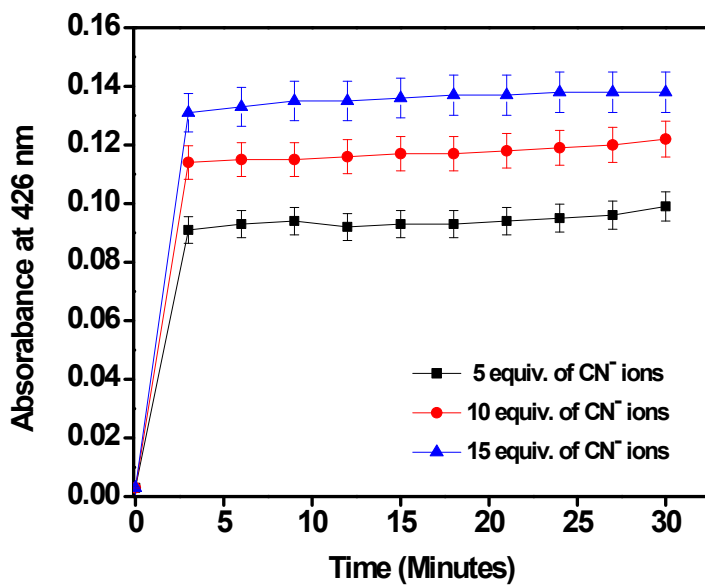


Fig. S16 Time Response of Ligand **L1** ($10\mu\text{M}$) upon addition of the different equivalent of CN^- ions

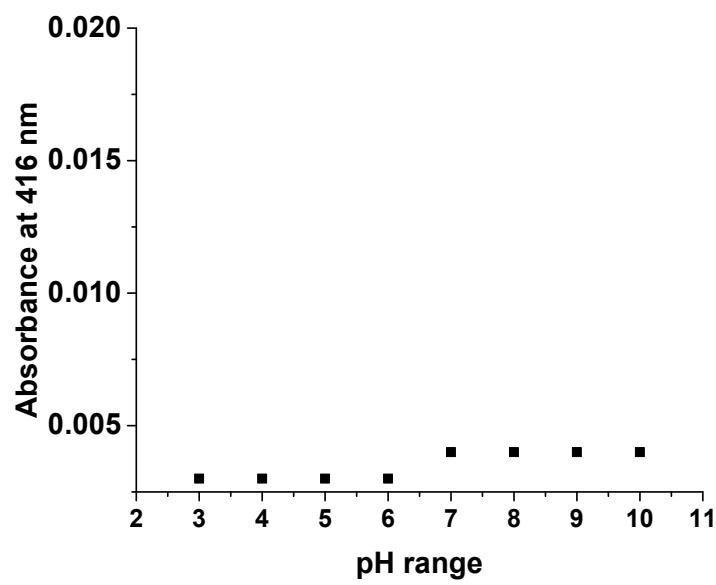


Fig. S17 pH response of ligand **L1** by varying pH from 3 to 10.

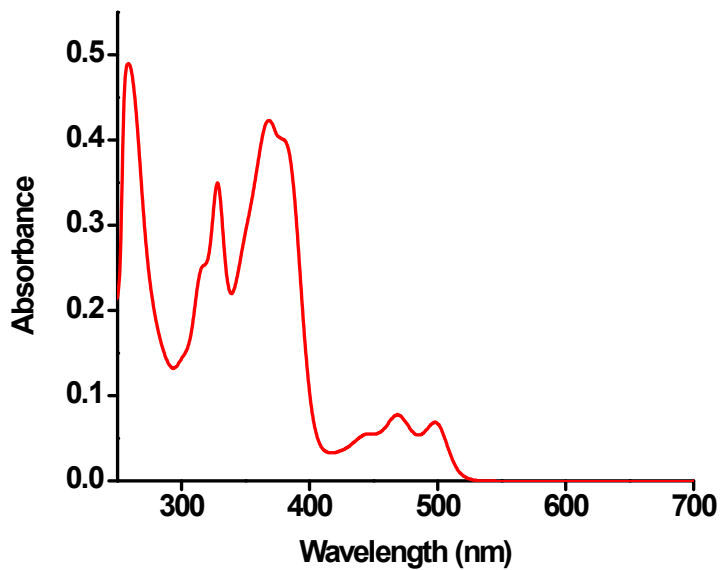


Fig. S18 UV-Vis absorption spectra of ligand **L2** (10 μ M) in DMSO.

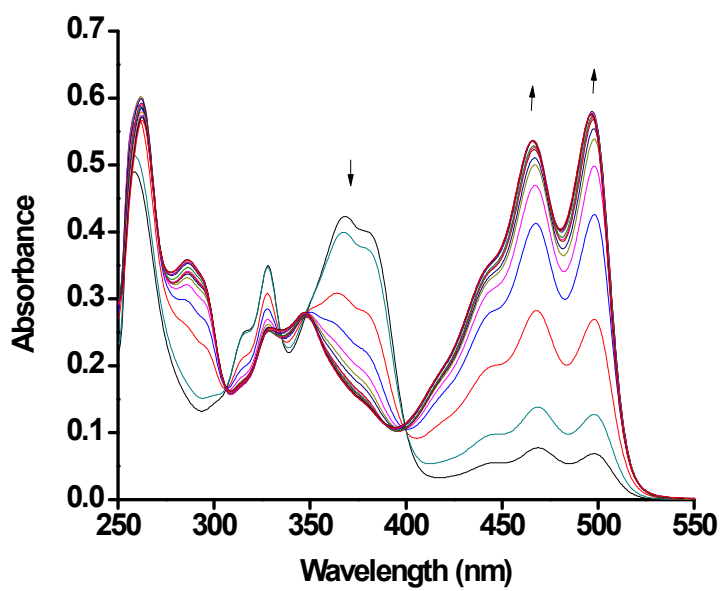


Fig. S19 UV-Vis absorption spectra of ligand **L2** (10 μ M) upon addition of 15 equiv. of CN⁻ ions.

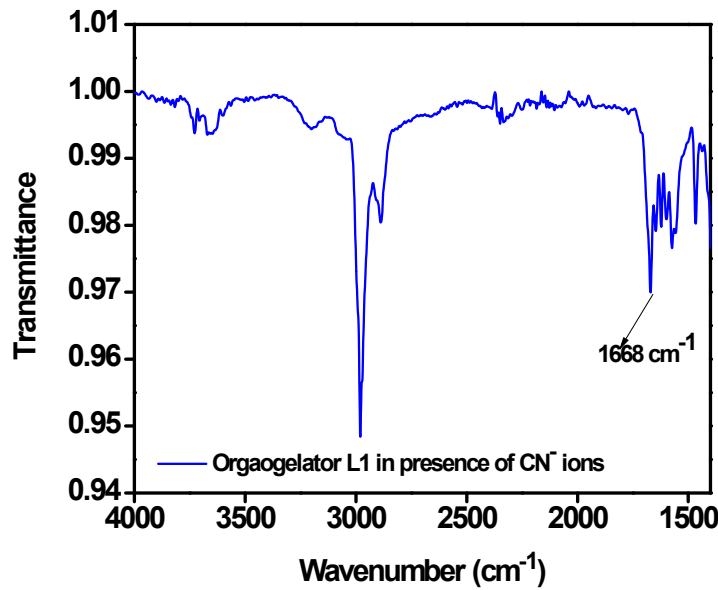
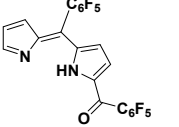
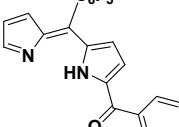
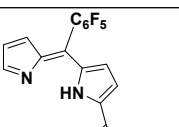
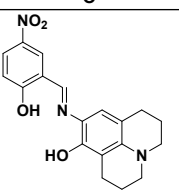
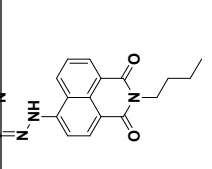
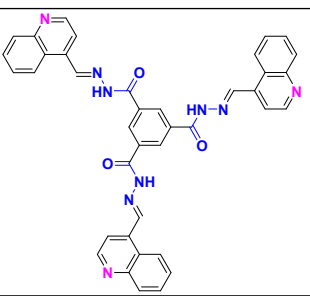


Fig. S20 FT-IR spectrum of the organogelator **L1** in the presence of CN^- ions.

Table 3: The comparison of the ligand **L1** for cyanide detection with other cyanide sensitive sensors.

Compounds	Sensing Method	Food Sample Analysis	Sensing with Organogelator	LOD	Reference
	Colorimetric changes	NO	NO	$105 \mu\text{M}$	¹
	Colorimetric changes	NO	NO	$20 \mu\text{M}$	²
	Colorimetric changes	NO	NO	$19.4 \mu\text{M}$	³
	Colorimetric changes	NO	NO	$4.5 \mu\text{M}$	⁴

	Colorimetric changes	NO	NO	3.6 μM	5
	Colorimetric changes	NO	NO	4.2 μM	5
	Colorimetric changes	NO	NO	7.1 μM	5
	Colorimetric changes	NO	NO	105 μM	6
	Colorimetric/Fluorescence changes	NO	NO	20.86 μM	7
	Colorimetric changes	YES	YES	1.5 μM	This Work

References:

- 1 H. J. Lee, S. J. Park, H. J. Sin, Y. J. Na and C. Kim, *New J. Chem.*, 2015, **39**, 3900–3907.
- 2 E. J. Song, S. Kim, G. J. Park, S. J. Park, Y. W. Choi, C. Kim and J. Kim, *Tetrahedron Lett.*, 2014, **55**, 6965–6968.
- 3 S. M. Kim, M. Kang, I. Choi, J. J. Lee and C. Kim, *New J. Chem.*, 2016, **40**, 7768–7778.
- 4 X. X. Ou, Y. L. Jin, X. Q. Chen, C. Bin Gong, X. B. Ma, Y. S. Wang, C. F. Chow and Q. Tang, *Anal. Methods*, 2015, **7**, 5239–5244.
- 5 Y. Ding, T. Li, W. Zhu and Y. Xie, *Org. Biomol. Chem.*, 2012, **10**, 4201–4207.
- 6 Y. J. Na, G. J. Park, H. Y. Jo, S. A. Lee and C. Kim, *New J. Chem.*, 2014, **38**, 5769–5776.

- 7 C. Rao, Z. Wang, Z. Li, L. Chen, C. Fu, T. Zhu, X. Chen, Z. Wang and C. Liu, *Analyst*, 2020, **145**, 1062–
1068.